IV Escola de Primavera de Transição e Turbulência
Universidade Federal do Rio Grande do Sul
Pontifícia Universidade Católica do Rio Grande do Sul
Porto Alegre, RS, 27 de setembro a 1º de outubro de 2004

WAVELET ANALYSIS OF EXPERIMENTAL TURBULENCE TIME SERIES

M. L. S. Indrusiak
S. V. Möller
Programa de Pós-Graduação em Engenharia Mecânica – PROMEC
Universidade Federal do Rio Grande do Sul – UFRGS
Rua Sarmento Leite, 425
90050-170 Porto Alegre, RS, Brasil
sperbindrusiak@via-rs.net
svmoller@vortex.ufrgs.br

Abstract. *Some wavelet analysis techniques applicable to experimental results of turbulence research studies are reviewed. The mathematical fundamentals are presented along with the procedures to apply the wavelet transform to the velocity and pressure discrete time series typical of wind tunnel turbulent flow research studies. Some results of studies with wakes of a single cylinder in cross flow as well as two and a row of cylinders, at both transient and permanent regime, are presented to illustrate the techniques.*

Keywords*. turbulence, transient flows, wavelets.*

1. Introduction

Wavelet techniques were introduced since 1930's by many researchers of diverse science fields, and unified in nineties by Yves Meyer, S. Mallat and others. In a historical point of view the first wavelet was created in the early 1910, where A Haar published a paper presenting an orthonormal basis alternative to Fourier basis, applicable where Fourier expansions do not converge (Haar, 1910)

Hubbard, 1998, wrote a review of the history of wavelets as a mathematical subject as well as a useful tool in applied sciences.

Meyer, 1993, in a more technical point of view, outlined the several paths that converge to the present state of the art in wavelet analysis techniques.

Since the past twenty years the wavelet transform found wide application in study of non-linear and intermittent phenomena, where Fourier spectral analysis is not suitable. From medical research to climate analysis, a wide range of science is experiencing an improvement by the recognition of the nonstationary (somewhat chaotic) nature of real phenomena and by the use of adequate analyzing tools to deal with this nonstationarity. The most widely used tool is the wavelet analysis, which decomposes a time series over a time frequency space, thus providing power distribution visualization along time and frequency, yielding an enhancement over Fourier analysis.

The band frequency filtering ability of the wavelet transforms allows the analysis of the features of the signal at almost any chosen frequency interval and bandwidth among the limits outlined by the uncertainty principle.

In fluid dynamics the phenomena, as well as the governing equations, are highly nonlinear and the assumption that the experimental data are at least weakly stationary is not always true. Wavelet analysis is a more flexible approach and allows an estimate of the error made as a result of violating the assumption of stationarity when using Fourier analysis.

This paper intends to be introductory to wavelet analysis applied to turbulence phenomena, remarkably in banks of tubes. The wavelet transform is first concisely presented by analogy to Fourier transform and then applied to the well-known phenomenon of the vortex street past a cylinder perpendicular to the flow. Flows past two and more cylinders are also analyzed.

2. Fundamentals

The Fourier transform of a function x(t), presented as a discrete time series, and its inverse are defined as:

$$x(f) = \frac{1}{2\pi}\sum_{0}^{T} x(t) e^{-ift} \tag{1}$$

and

$$x(t) = \sum_{-\infty}^{\infty} x(f)\, e^{i\,f\,t} \tag{2}$$

The Fourier spectrum gives the energy distribution of the signal in the frequency domain and is evaluated over the entire time interval:

$$P_{xx}(f) = |x(f)|^2 \tag{3}$$

More suitable for evaluate the spectral energy distribution of the signal is the power spectral density function (PSD) which is the Fourier spectrum (Eq. (3)) smoothed over frequency intervals and over an ensemble of estimates in order to deal with the random error (Bendat and Piersol, 1971). In practice the computation can be performed, as suggested by Einstein, 1912, by doing the Fourier transform of the autocorrelation function:

$$P_{xx}(f) = \int_{-\infty}^{\infty} \left(\lim_{T\to\infty} \frac{1}{T} \int_0^T x(t)\, x(t+\tau)\, dt \right) e^{-i\,2\pi f\,\tau}\, dt \tag{4}$$

The Fourier transform of the cross correlation function of the signals x(t) and y(t) is a complex function called cross spectral density function (CSD).

The Fourier spectral analysis, as well as correlation methods, is adequate to study permanent signals but not to deal with transitory processes at different scales. An attempt to deal with transient series is the windowed Fourier transform, which performs the Fourier transform on a sliding segment of the entire time series. However, due to the aliasing of high and low frequency components that do not fall within the frequency range of the window, the windowed Fourier transform is inaccurate for time-frequency localization of transient features (Torrence and Compo, 1998).

Wavelet analysis arises from the idea of stretching and compressing the window of the windowed Fourier transform, according to the frequency to be localized, thus allowing the definition of all scales of interest in time and frequency domain.

While the Fourier transform uses trigonometric functions as basis, the bases of wavelet transforms are functions named wavelets.

A wavelet is a finite energy function, $\psi(t)$, with a zero average, which satisfies the admissibility condition:

$$C_\psi = \int_0^\infty \frac{|\psi(f)|^2}{f} df < \infty, \tag{5}$$

where $\psi(f)$ is the Fourier transform of the wavelet.

The wavelet function is also called mother wavelet, because it generates an entire set of wavelet basis:

$$\psi_{a,b}(t) = \frac{1}{\sqrt{a}}\, \psi\left(\frac{t-b}{a}\right),\ a, b \in R,\ a > 0 \tag{6}$$

The parameters a and b are respectively scale and position coefficients.

The choice of a wavelet function to a given application has infinite possibilities, although only a few are of practical interest. There is not a general rule, but a good hint is to choose a wavelet with a shape similar to that of the function to be analyzed. Nevertheless the results of different wavelets applied to the data should be compared, in order to assure a good choice.

The continuous wavelet transform (CWT) of a function x(t) and its inverse transform are given by:

$$Wx(a,b) = \int_t x(t)\, \psi_{a,b}(t)\, dt \tag{7}$$

and

$$x(t) = \frac{1}{C_\psi} \int_b \int_a Wx(a,b)\, \psi_{a,b}(t)\, \frac{da\, db}{a^2} \tag{8}$$

The respective wavelet spectrum is defined as:

$$P_{xx}(a,b) = |Wx(a,b)|^2 \tag{9}$$

The complex cross wavelet spectrum of two functions x(t) and y(t) is defined as:

$$P_{xy}(a,b) = Wx(a,b)Wy^{*}(a,b) \tag{10}$$

where Wy*(a,b) is the complex conjugate of the CWT of y(t).

The scale and position parameters a und b above are related to the frequency and time of the analyzed function.

While the Fourier power spectrum, Equation (3), gives the energy for each frequency over the entire time domain, in the wavelet spectrum, Equation (9), the energy is related to each time and scale (or frequency). This characteristic of the wavelet transform allows the representation of the distribution of the energy of the transient signal over time and frequency domains.

The discrete wavelet transform (DWT) is, according to Percival and Walden, 2000, a judicious sub sampling of CWT, dealing with just dyadic scales, and is given by:

$$D(j,k) = \sum_{t} x(t)\psi_{j,k}(t) \tag{11}$$

and its inverse transform is:

$$x(t) = \sum_{j}\sum_{k} D(j,k)\psi_{j,k}(t) \tag{12}$$

where the scale and position coefficients (j, k) are dyadic sub samples of (a, b).

Taking $a=2^j$ and $b=k2^j$ the set of wavelet functions are generated by:

$$\psi_{j,k}(t) = 2^{\frac{-j}{2}}\psi\left(2^{-j}t-k\right), \quad j,k \in N \tag{13}$$

The discrete wavelet spectrum is defined by:

$$P_{xx}(j,k) = |D(j,k)|^2 \tag{14}$$

The Fourier transform of a finite series gives only a finite number of coefficients, depending on the length of the time series, and therefore neglects the coefficients related to the higher frequencies. Anyway, these frequencies are already filtered at the acquisition process, to prevent aliasing. In the wavelet transform of a finite series, the length of the series also restricts the number of computable coefficients but, unlike the Fourier transform, the remaining coefficients are related to the lower frequencies, including the mean value of the signal, and cannot be disregarded. In practice, the DWT of a series with more than 2^J elements is computed for $1 \le j \le J$, being J a convenient arbitrary choice. The remaining part of the signal, containing the mean values for a scale J, is given by:

$$A(J,k) = \sum_{t} x(t)\phi_{J,k}(t) \tag{15}$$

where $\phi(t)$ is the scaling function associated to the wavelet function and:

$$\phi_{j,k}(t) = 2^{\frac{-j}{2}}\phi\left(2^{-j}t-k\right) \tag{16}$$

The inverse transform of a discrete time series with acquisition frequency Fs is done by:

$$x(t) = \sum_{k} A(J,k)\phi_{J,k}(t) + \sum_{j\le J}\sum_{k} D(j,k)\psi_{j,k}(t) \tag{17}$$

where the first term is the approximation of the signal at the scale J, which corresponds to the frequency band $[0\ ,\ Fs/2^{J+1}]$ and the inner sum of the second term are details of the signal at the scales j ($1 \le j \le J$), which corresponds to frequency bands $[Fs/2^{j+1}\ ,\ Fs/2^j]$

Figure (1a) illustrates the pyramid algorithm (Mallat, 1999) for computation of the DWT. A new form of transformation, called discrete wavelet packed transform (DWPT), is obtained by means of a simple modification of the algorithm, illustrated at figure (1b), where each detail series is wavelet transformed in two series, with respectively lower and upper half width frequency interval, allowing, for each level j, the split of the frequency interval of the original series [0 , f/2] into 2^j successive intervals of same bandwidth.

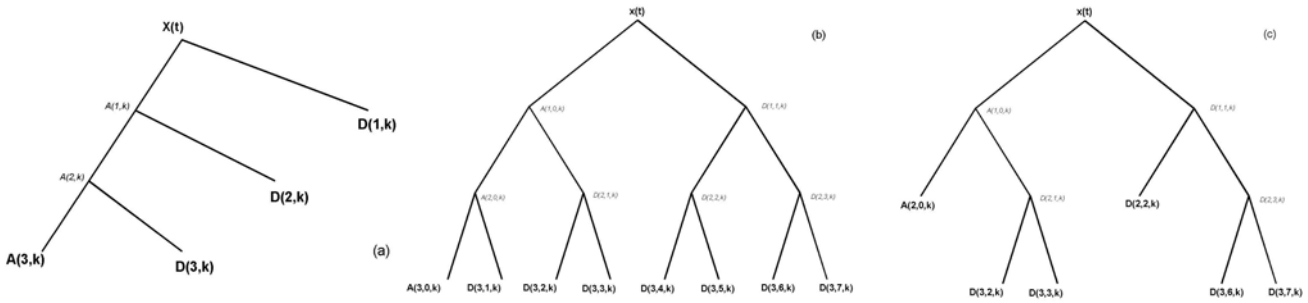

Figure 1: Representation of the pyramid algorithm for (a) DWT ; (b) DWPT and (c) another choice for DWPT

The main characteristic of the DWPT is that it allows a multiresolution analysis of the signal. Therefore any admissible binary tree can be chosen for the representation of the signal in the wavelet space, with unequal frequency bandwidths, according to the analysis to be done. An admissible tree is any binary tree where each node has either 0 or 2 branches. Figure (1c) shows an example of admissible DWPT tree.

3. Experimental technique

The test section, shown in Fig. (2), is a 1370 mm long rectangular channel, with 146 mm height and a width of 193 mm. Air, at room temperature, is the working fluid, driven by a centrifugal blower, passed by a diffuser and a set of honeycombs and screens, before reaching the test location with about 1 % turbulence intensity. Before the measurement location, a Pitot tube is placed at a fixed position to measure the steady reference velocity of the measurements.

For measurements of velocity and velocity fluctuations, DANTEC *StreamLine* constant temperature hot wire anemometers were applied, with single straight probes and a double (X) probe. The pressure fluctuations were acquired with a ENDEVCO piezo-resistive pressure transducer, mounted inside the tube and connected to a pressure tap drilled in a nylon support adjusted to the tube inner wall (Goulart, 2004). The experiments in the transient regime were performed by simply turning the blower on, being the measurement equipments previously set to operate and data acquisition started.

Data acquisition of velocities and pressure fluctuations were performed with a 12 bit Keithley DAS-58 A/D-converter board with a sampling frequency of 8 kHz, and a low pass filter set at 3 kHz for velocity signals and 3.6 kHz for pressure signal.

Analysis of uncertainties in the results has a contribution of 1.4 % from the measurement equipments (including hot wire and A/D converter). The mean error of the determination of the flow velocity with a hot wire was about 3.4%. Velocity fluctuations in the main flow direction were obtained with a mean error of 15%, while the transverse component had an error of about 30%.

The Fourier and wavelet transforms are computed with the Matlab 5.3 software.

The Daubechies “db20” functions were used to the bases of the discrete wavelet transforms and the Morlet function was used for the basis of the continuous transforms.

4. Results

4.1. Transient Vortex Street

The vortex street is a well-known example of flow with coherent structures at a characteristic frequency. But what is the behavior of the wake in a transient flow and what does really mean the predominant frequency of the wake are open questions.

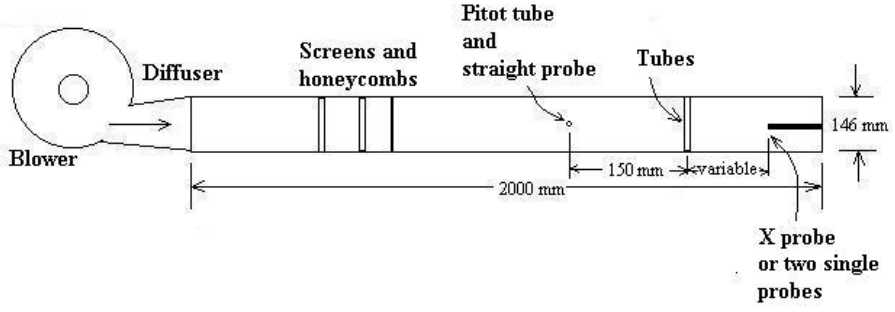

Figure 2: Schematic view of the test section

As an attempt to answer these questions an experiment was performed with a single tube positioned perpendicularly to the wind tunnel main axis, and velocity and pressure measurements were made with the blower departing from rest, running until to the permanent velocity, thus producing a vortex street in a transient regime. There was applied a straight and an x hot wire probes, as explained at Section 3.

The tube diameter is 0.032m; the Reynolds number when the flow achieves the permanent regime is $3.8 \cdot 10^4$, with a prevailing frequency of 95 Hz (Strouhal number = 0.22).

Figure (3) shows the two time series acquired simultaneously: the incident reference velocity, obtained with the hot wire probe positioned 0.15 m upstream the tube section and the wake velocity, obtained 0.10 m downstream the tube section.

Figure (4) is the continuous wavelet spectrum of the wake velocity computed according to Eq. (9), showing the energy distribution of the signal over time and frequency. The evolution of the wake in time, frequency and also in energy intensity is observed at the figure. The almost homogeneous increase of energy concerned to the transient wake is very clear, as well as the energy and frequency oscillation at the stationary part of the wake.

Any slice of the graph, parallel to frequency-energy plane, will show an instantaneous spectral energy distribution of the signal, whereas if the slice is parallel to time-energy plane, the energy oscillation along time for a chosen frequency will be seen.

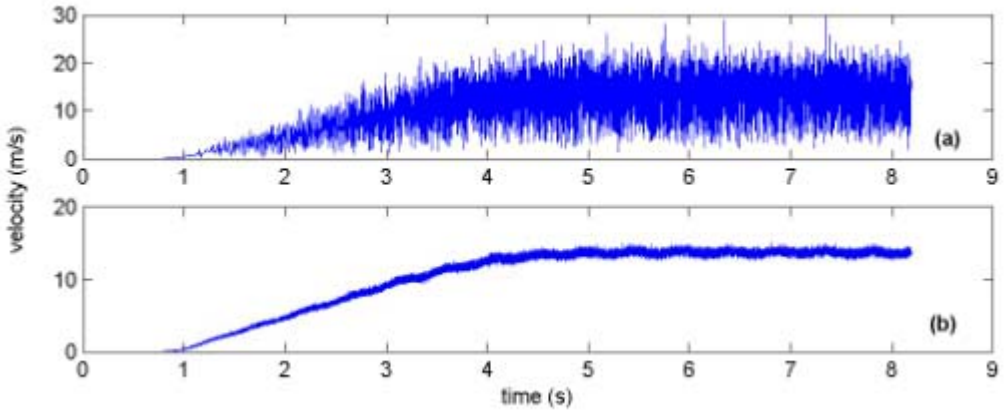

Figure 3: Velocity signals acquired in a transient regime: (a) wake velocity and (b) incident reference velocity.

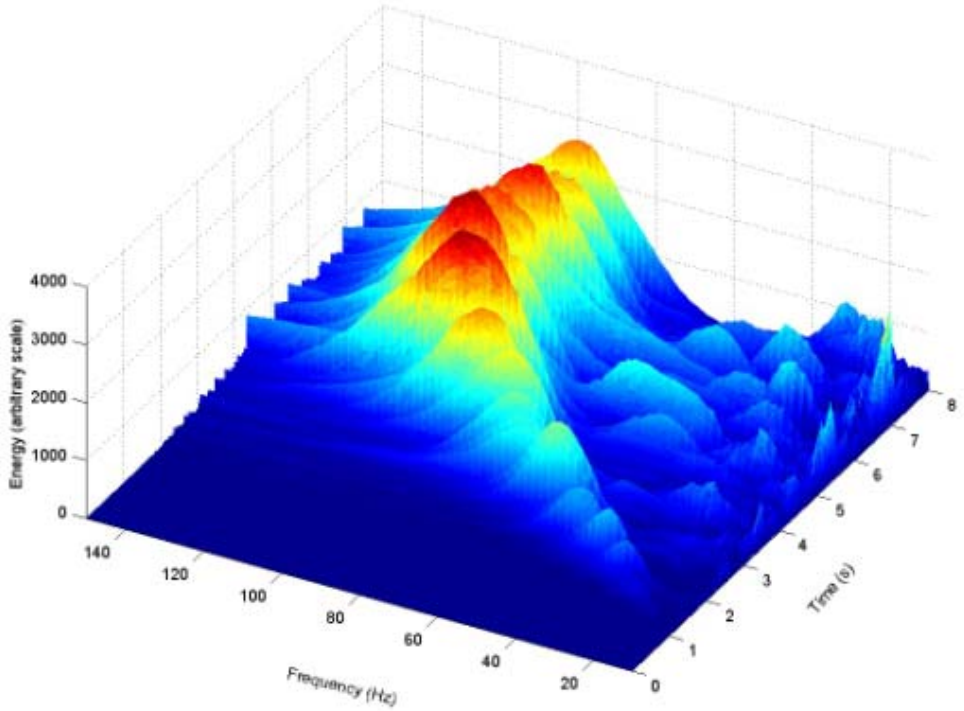

Figure 4: Continuous wavelet spectrum of the axial velocity signal acquired in the transient regime (fig. 3-a), in the wake of the cylinder.

To evaluate the frequency and energy oscillation of the wake, two signals were analytical generated: (a)a signal with a linear increasing frequency (a linear chirp) and a continuously increasing energy and (b)a pure sinusoidal signal with a frequency of 87 Hz, the same value of the main frequency of the permanent part of the wake shown at Fig (5). Their wavelet spectra are displayed respectively at Fig (5a) and Fig (5b) and their observation certifies that the oscillations observed at the wake are inherent to the phenomenon observed and not artifacts of the transform.

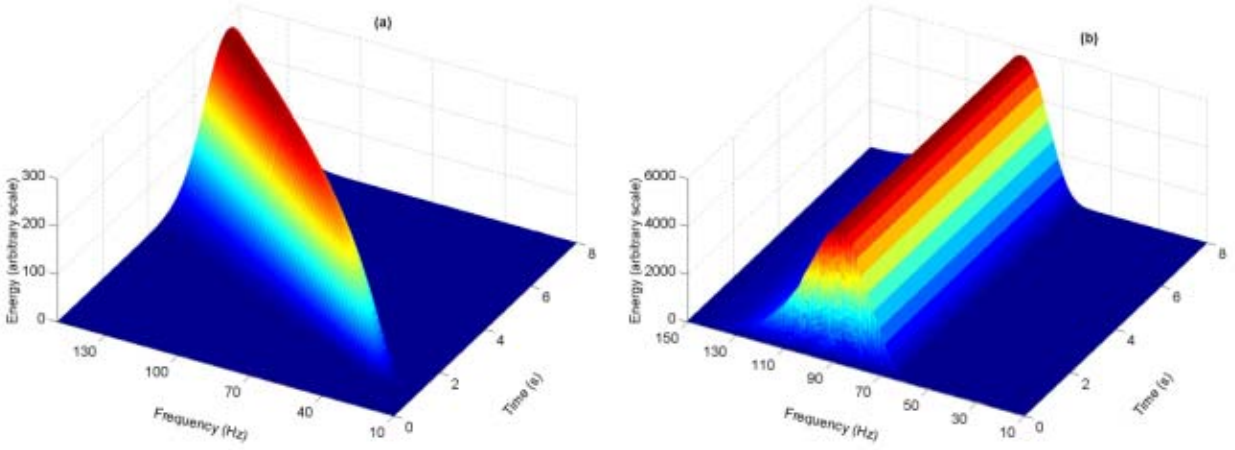

Figure 5: (a) Continuous wavelet spectrum of a linear chirp. (b) Continuous wavelet spectrum of a sine function.

4.2. Wake of two side-by-side circular cylinders

The behaviour of the flow past two side-by-side circular cylinders has been studied by many authors, e. g. Sumner et al., 1999, Zhang and Zhou, 2001, Xu et al, 2003, at several pitch to diameter ratios. At intermediate ratios they observed a transient, bistable wake, characterized by a narrow near-wake region behind one of the cylinders and a wide one behind the other, with an intermittent switching among them. Alam et al., 2003, applied wavelet analysis to the switching phenomenon, characterizing an in phase and an out of phase regimes of the cylinder wakes.

In the present work, two cylinders were assembled at test section, Fig. (1), with a pitch to diameter ratio of 1.26. Two hot wire straight probes were applied, aligned with the tangents to the cylinders at the gap between them. The results for positions 30 mm and 60 mm downstream the cylinder centre line are at Fig. (6) and (9).

Figure (6) shows a characteristic bistable flow, with a mode interchange around 5 seconds and several velocity peaks along the signal, suggesting a tendency for change between the two modes. The respective continuous wavelet spectra are at figure (7) and show an increment of the energy at low frequencies for the part of the signal with higher mean velocity, independently of the mode. Figure 8 shows the result of the application of the DWT and then the reconstruction of the signals by frequency intervals, according to Eq. (17), first sum for the lower frequency interval and second inner sum for the others. Each figure shows, at one sight, that the behaviour of the signals are distinct for each mode at all frequency intervals.

The signals acquired 60 mm downstream the cylinder centreline, Fig. (9), corresponds apparently to a flow with only one mode, with the mean value of velocities being approximately constant along the acquisition period. But the wavelet spectra of the signals, Fig. (10), show an ever more pronounced bistable behaviour than that presented by the 30 mm downstream signals, with a mode change around 4 seconds.

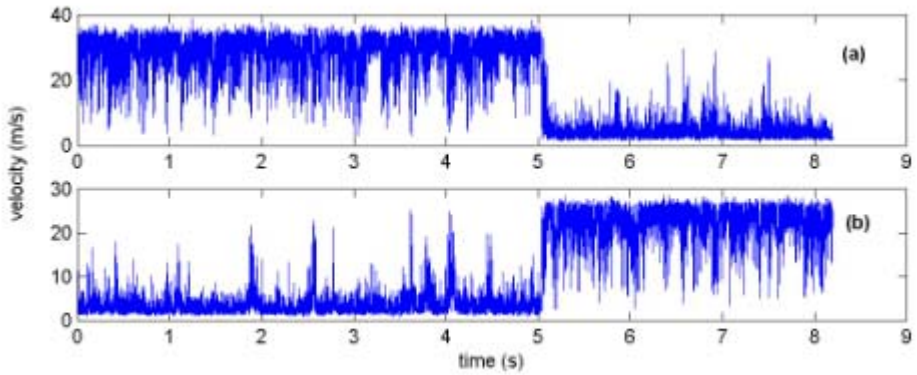

Figure 6: Velocity signals acquired in the gap jet, 30 mm downstream the centreline of the cylinders, showing the bistable effect.

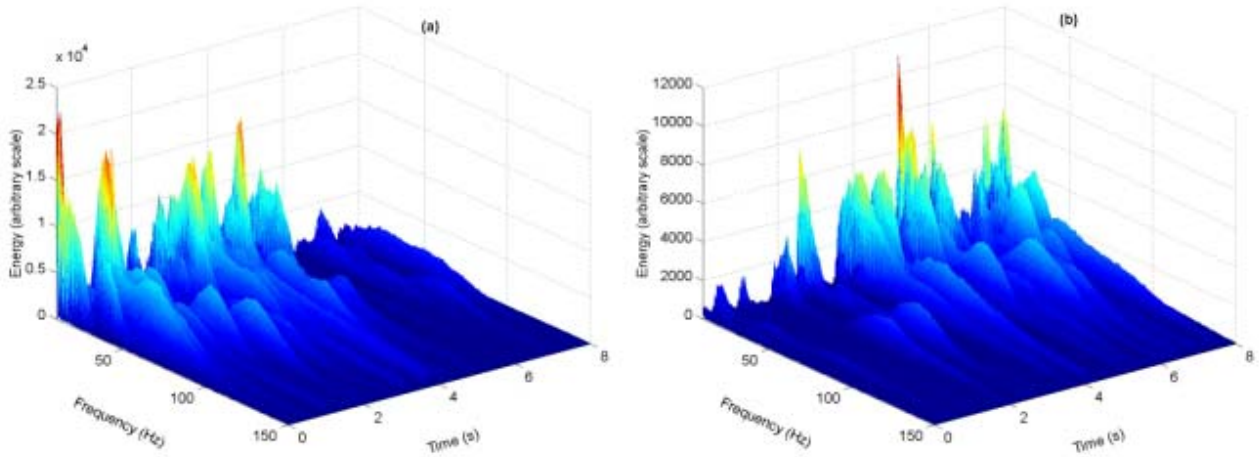

Figure 7: Continuous wavelet spectrum of the signals of Fig. (6). The bistable flow is also characterized by the energy distribution at the lower frequencies.

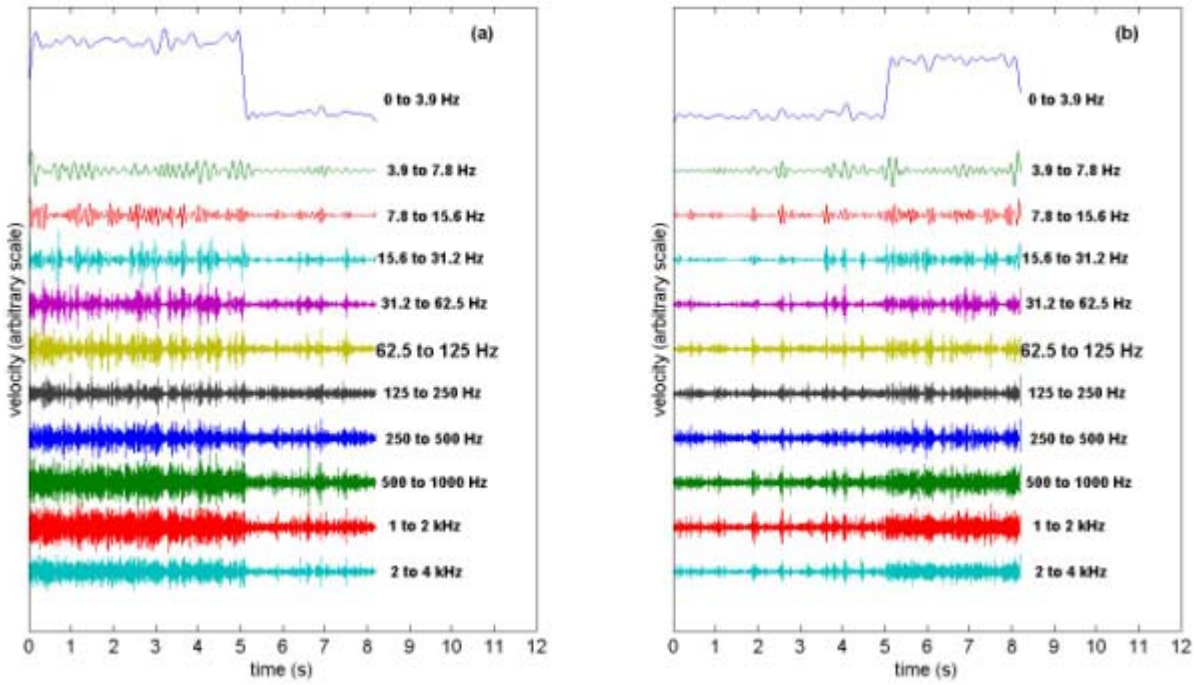

Figure 8: The signals presented at Fig. (6), discrete wavelet transformed and reconstructed for each frequency level.

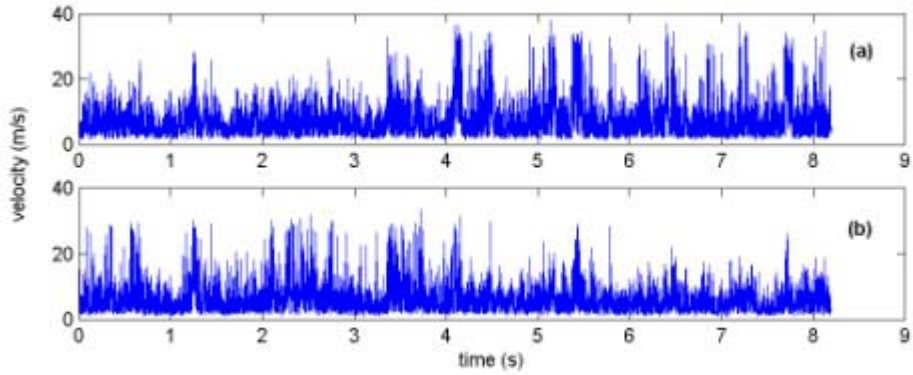

Figure 9: Velocity signals acquired in the gap jet, 60 mm downstream the centreline of the cylinders.

The wavelet cross-spectra of the 30 and 60 mm downstream signals are presented at Fig. 11. The 30 mm downstream signals cross spectrum shows an interval around 3.5 and 5 seconds at frequencies lower than 100 Hz, just prior to the mode change, with more coherence than that of the neighbouring instants. Diversely, the cross wavelet spectrum of the 60 mm downstream signal seems to have an almost uniformly distributed coherence, with higher values for frequencies lower than 100 Hz and a special region around 4 to 6 seconds with more coherence, which seems to indicate a mode transition behaviour. Both signals show a slight persistent coherence at approximately 70 Hz.

4.3. Wakes of a row of cylinders

Tubes arranged inline perpendicular to the flow are a usual geometry, e.g. offshore structures and grids, and can be view also as a first approach for more complex arrangements like tube banks, encountered in many engineering applications, like energy and process industry. The flow, undisturbed prior to the first row tubes, is set by them and then travels through the bank. In the present work, a single row of five tubes was assembled at test section, Fig. (1), with a pitch to diameter ratio of 1.26. Two hot wire straight probes were applied, parallel to the wind tunnel main axis, aligned with the tangents to the central (probe a) and first lateral (probe b) cylinders at the gap between them. Measurements were made 30 and 60 mm downstream the cylinder centreline.

The discrete wavelet transform was applied to the velocity signals for position 30 mm. The inverse transformed approximations for 0 to 7.8 Hz frequency interval were computed according to the first right term of Eq. (17). The results are at Fig. (12-a) and show a strong negative correlation among the two velocity signals, also corroborated by the cross correlation presented at Fig. (12-b).

The PSD function of the signal of probe a and the respective continuous wavelet spectrum are presented at Fig. (13). The peak near 200 Hz at power spectrum seems to be a vortex frequency but at the wavelet spectrum one can see that there is only a narrow region, near 4 seconds, where a significant concentration of energy at 200 Hz occurs.

The Fourier and wavelet spectra for the velocity signals acquired at position 60 mm are presented respectively at Fig. (14) and (15). While the PSD of both signals show a single peak around 200 Hz, the wavelet spectra of the same signals show that the wake frequency can oscillate around the main value, as at Fig. (15-a), and also that the energy distribution at the wake can be very intermittent, as at Fig. (15-b).

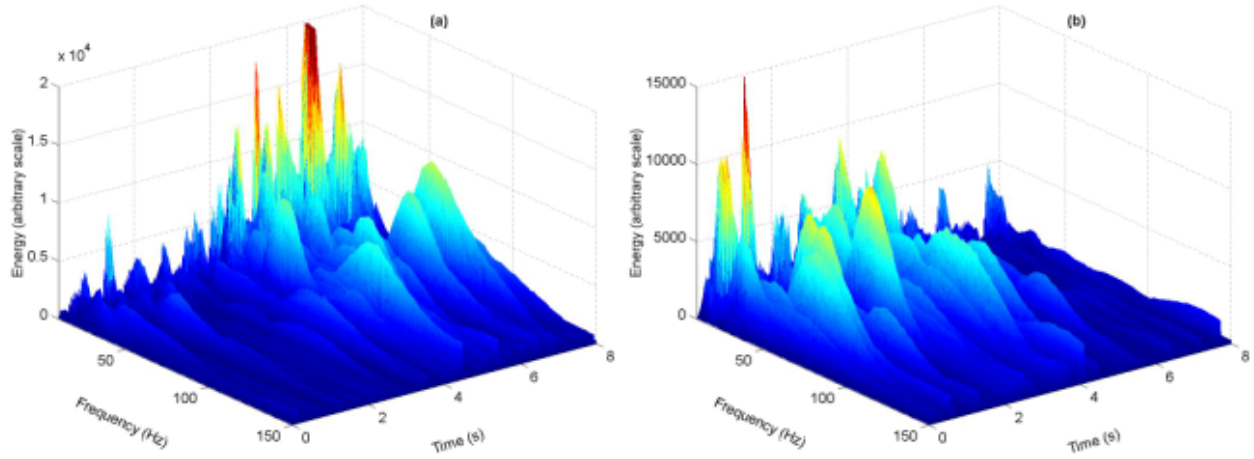

Figure 10: The continuous wavelet spectra of the signals of Fig. (9).

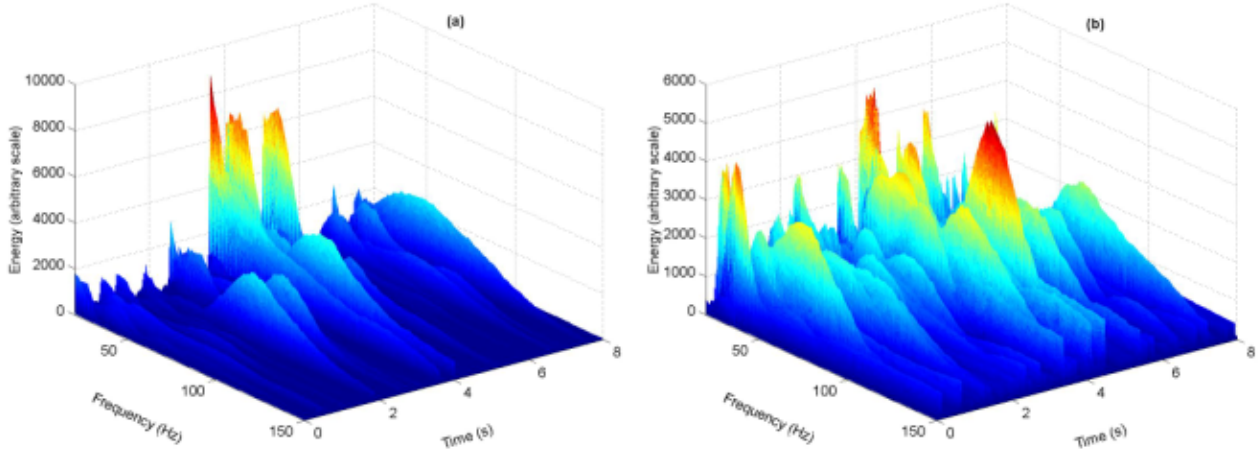

Figure 11: (a) Cross wavelet spectra of signals of Fig. (6). (b) Cross wavelet spectra of signals of Fig. (9).

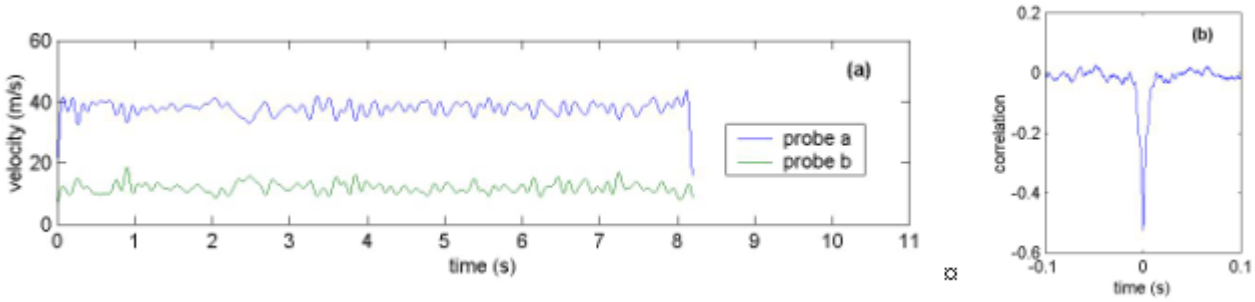

Figure 12: (a) Wavelet approximations for 0 to 7.8 Hz of the velocity signals acquired 30 mm downstream the tube row. (b) Cross correlation function of the velocity signals.

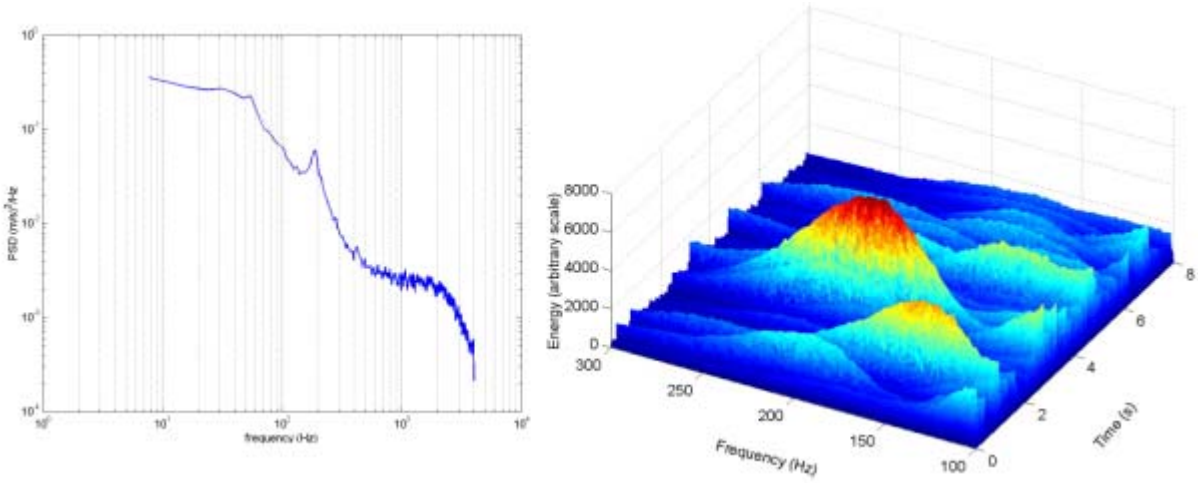

Figure 13: PSD and wavelet spectrum of the velocity signal of the probe a, acquired 30 mm downstream the tube row.

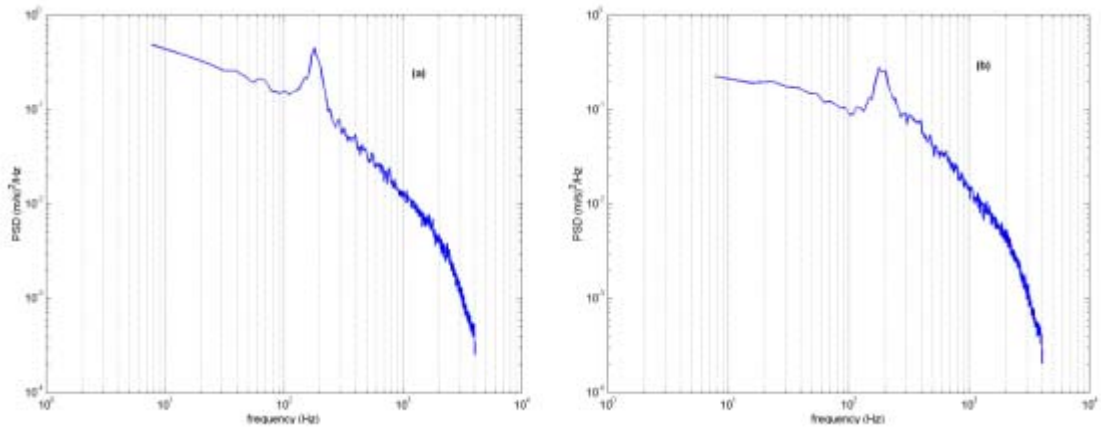

Figure 14: Fourier power spectra of the two velocity signals acquired 60 mm downstream the tube row.

5. Conclusions

The selected results presented at this article aimed to show that the wavelet analysis is a valuable complementary tool to Fourier analysis. While Fourier spectral analysis as well as correlation analysis can deal with only stationary series, whose mean and RMS values do not change with the time interval, wavelet analysis do not have that restriction at all.

Nevertheless, the application of the wavelet methods is not so straightforward as the Fourier ones. That may be due to:

a) the choice of a more suitable wavelet function offers many possibilities.
b) there are several transforms, each one with characteristic properties.
c) there are various representation forms of the wavelet results.

Even when the signal is or is presumed to be stationary, the wavelet analysis can be useful in confirming the stationary assumption or to show how slight or strong are the energy oscillations of the signal along time. Their concurrent use with the Fourier analysis allows a more complete observation of the studied phenomena.

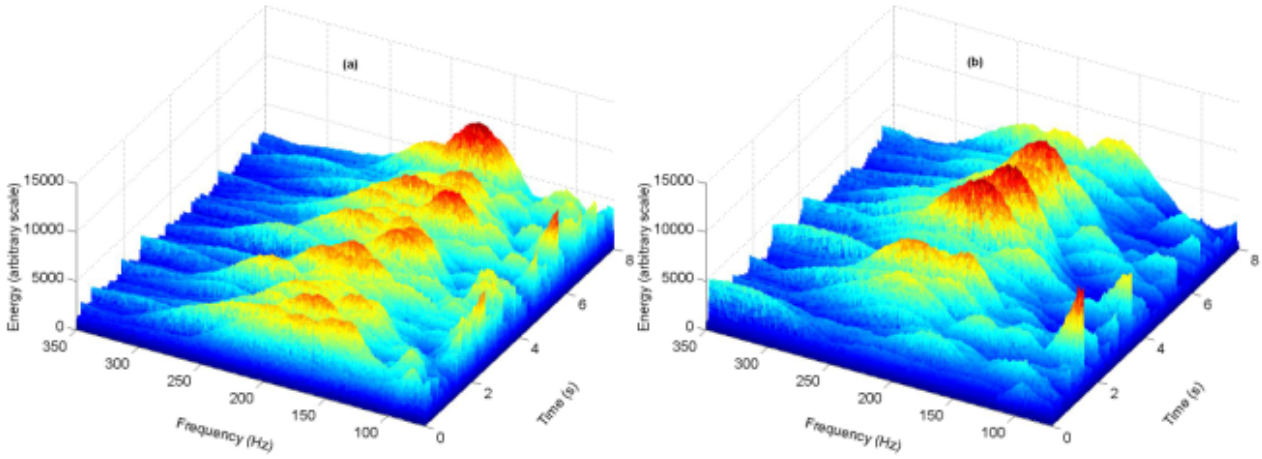

Figure 15: Wavelet spectra of the same signals of Fig. (14).

6. Acknowledgements

Authors gratefully acknowledge the support by the CNPq - Brazilian Scientific and Technological Council, under the grants 414216/90-3, 400180/92-8 and 520986/1997-0.

7. References

Alam, M. M., Moriya, M. and Sakamoto, H., 2003, Aerodynamic characteristics of two side-by-side circular cylinders and application of wavelet analysis on the switching phenomenon, Journal of Fluids and Structures, v. 18, pp 325-346.

Bendat, J. S. and Piersol, A. G., 1971, Random Data: Analysis and Measurement Procedures, Wiley-Interscience.

Einstein, A., 1914, Eine Methode zur statistischen Verwertung von Beobachtungen scheinbar unregelmäßig quasiperiodisch verlaufender Vorgänge, The collected papers of Albert Einstein, Vol. 4, Princeton University Press.

Goulart, J. N., 2004, "Estudo experimental dos campos de pressão e velocidade em bancos de tubos com a utilização de defletores"- Dissertação de Mestrado (Experimental study of pressure and velocity fields in tube banks with baffle plates), Universidade Federal do Rio Grande do Sul.

Haar A., 1910, Zur Theorie der Orthogonalen Funktionensystheme, Math. Annal., 69, 331-371.

Hubbard, B. B., 1998, The World According to Wavelets, AK Peters.

Mallat, S., 1999, A Wavelet Tour of Signal Processing, Academic Press.

Meyer, Y., 1993, Wavelets: algorithms and applications, SIAM.

Percival, D. B. and Walden, A. T., 2000, Wavelet Methods for Time Series Analysis, Cambridge University Press.

Sumner, D., Wong, S. S. T., Price, S. J. and Païdoussis, 1999, Fluid behaviour of side-by-side circular cylinders in steady cross-flow, Journal of Fluids and Structures, v. 13, 309-338.

Torrence, C. and Compo, G. P., 1998, A Practical Guide to Wavelet Analysis. Bulletin of the American Meteorological Society.

Xu, S. J., Zhou, Y. and So, R. M. C., 2003, Reynolds number effects on the flow structure behind two side-by-side cylinders, Physics of Fluids, v.15, n. 5, pp. 1214-1219.

Zhang, H. J. and Zhou, Y., 2001, Effect of unequal cylinder spacing on vortex streets behind three side-by-side cylinders, Physics of Fluids, v. 13, n. 12, pp. 3675-3686.